

Electronic Supplementary Information (ESI)

Crystal Reconstruction and Defects Healing Enabled High-quality Sb₂Se₃ Films for Solar Cell Applications

Qi Zhao,^a Bo Che,^a Haolin Wang,^a Xiaoqi Peng,^a Junjie Yang,^a Rongfeng Tang,^a Changfei Zhu,^a and Tao Chen^{*a}

a. Hefei National Research Center for Physical Sciences at the Microscale, CAS Key Laboratory of Materials for Energy Conversion, Department of Materials Science and Engineering, School of Chemistry and Materials Science, University of Science and Technology of China, Hefei, 230026, China.

*Corresponding authors: Tao Chen

E-mail: tchenmse@ustc.edu.cn

This file includes:

Supplementary note S1

Figure S1 to S6

Table S1 to S7

References

Supplementary Note

Note 1

Principles of Deep-level Transient Spectroscopy

We conducted deep-level transient spectroscopy (DLTS) to detect the deep-level defects properties and the defect level is identified from DLTS signal using Fourier deconvolution algorithm. The active energy (E_a , E_C-E_T or E_T-E_V) and capture cross section of electron traps and hole traps can be calculated by the Arrhenius Equations (1) and (2),

$$\ln(\tau_e v_{th,p} N_V) = \frac{E_T - E_V}{k_B} \frac{1}{T} - \ln(X_p \sigma_p) \#(1)$$

$$\ln(\tau_e v_{th,n} N_C) = \frac{E_C - E_T}{k_B} \frac{1}{T} - \ln(X_n \sigma_n) \#(2)$$

where τ_e , N_V , N_C , E_T , E_V , and E_C are emission time constant, valence band state density, conduction band state density, trap energy level, valence band, and conduction band, respectively. $v_{th,n/p}$, $X_{n/p}$, and $\sigma_{n/p}$ are thermal velocity, entropy factor, and capture cross-section for electron and hole, respectively. E_a can be obtained from the slope of the corresponding line, and the σ can be obtained from the y-intercept of the lines. The trap concentration (N_T) can be acquired from Equation (3):

$$N_T = 2N_S \frac{\Delta C}{C_R} \#(3)$$

where N_S is the shallow donor concentration, C_R is the capacitance under reverse bias, while ΔC represents the amplitude of transient capacitance.

The product of the capture cross section and the defect density ($\sigma \times N_T$) is considered as an important parameter for the intuitive evaluation of the carrier lifetime, and the relationship follows the following Equation (4):

$$\tau_{trap} = \frac{1}{v\sigma N_T} \#(4)$$

where v is the thermal velocity of electric charge.^{1,2}

Supplementary Figure

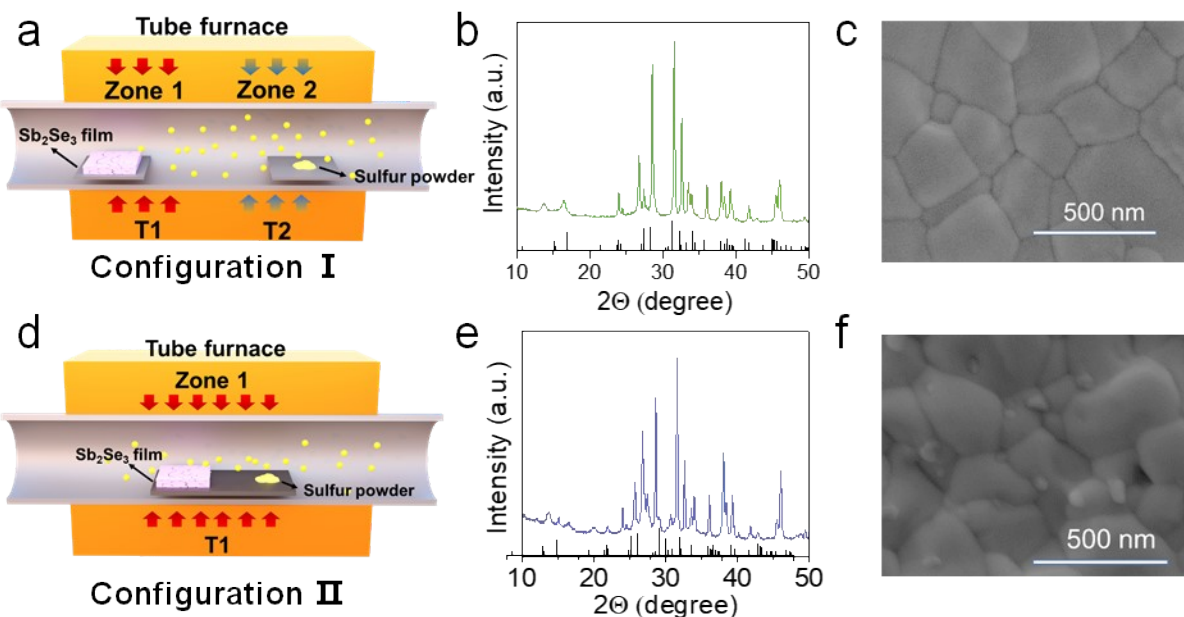


Fig. S1. Characterization of structure and surface morphology of the films. XRD pattern of the Sb_2Se_3 films sulfurized using b) configuration I and e) configuration II; Surface SEM images of the Sb_2Se_3 films sulfurized using b) configuration I and e) configuration II.

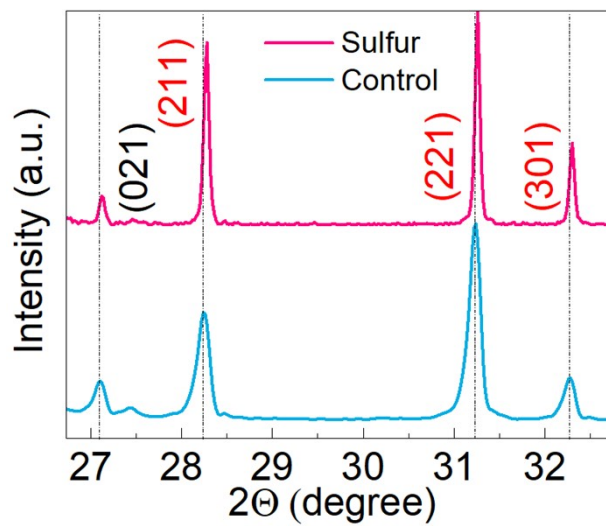


Fig. S2. Magnified view of the (021), (211),(221) and (301) XRD peaks of the films.

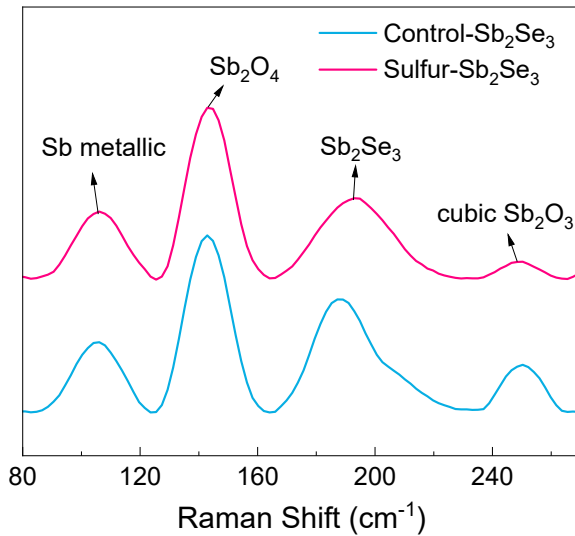


Fig. S3. Raman spectra of the Control-Sb₂Se₃ and Sulfur-Sb₂Se₃ films.

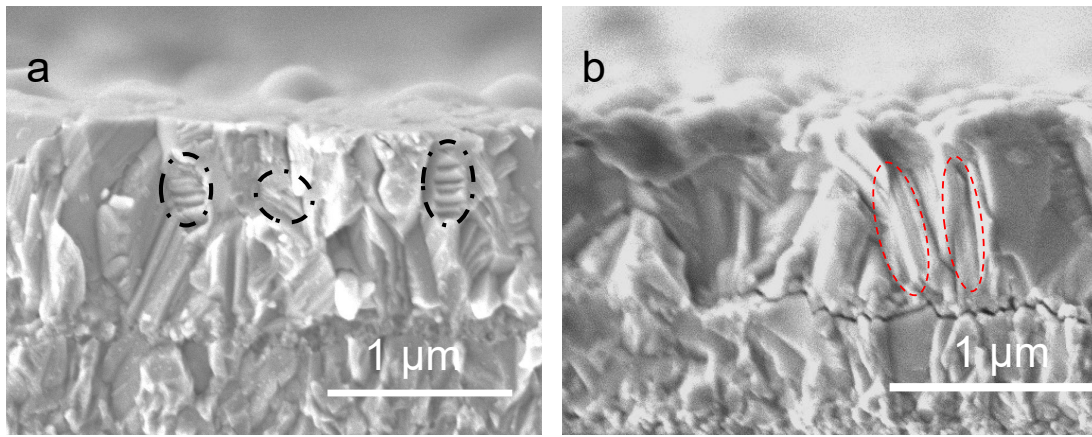


Fig. S4. The cross-sectional SEM image of the films. a) Control-Sb₂Se₃ films, b) Sulfur-Sb₂Se₃ films.

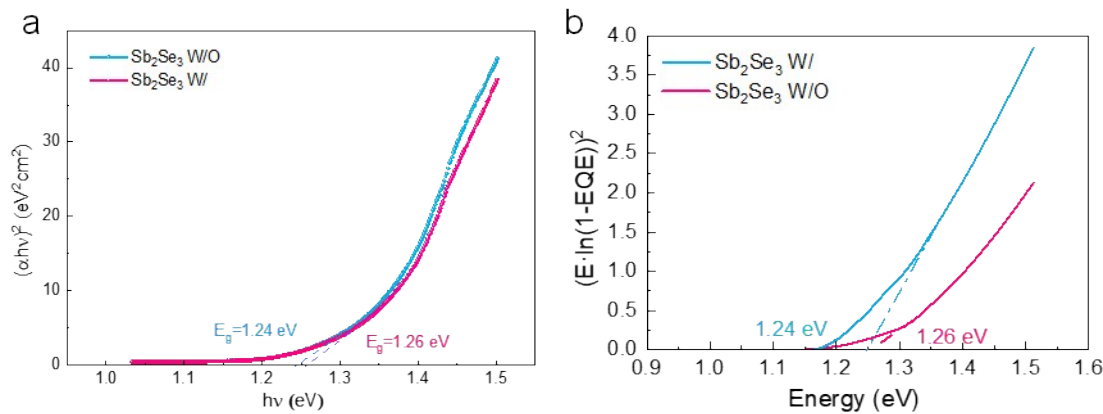


Fig. S5. UV-visible absorption characterization of the films. a) plot of $(\alpha h\nu)^2$ versus $(h\nu)$ of Sb₂Se₃ films. b) Bandgap value extracted from EQE spectra.

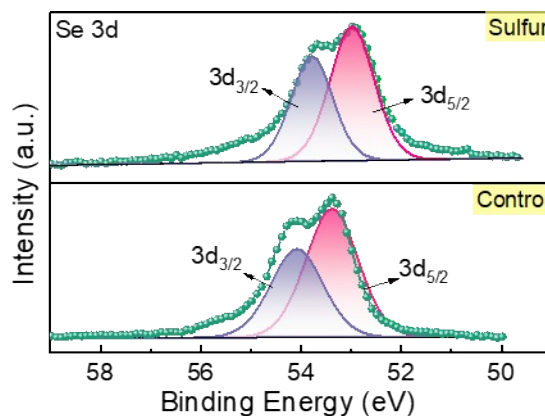


Fig. S6. Surface composition of the films. Analysis of the surface chemical states of Control-Sb₂Se₃ and Sulfur-Sb₂Se₃ films for Se 3d XPS peaks.

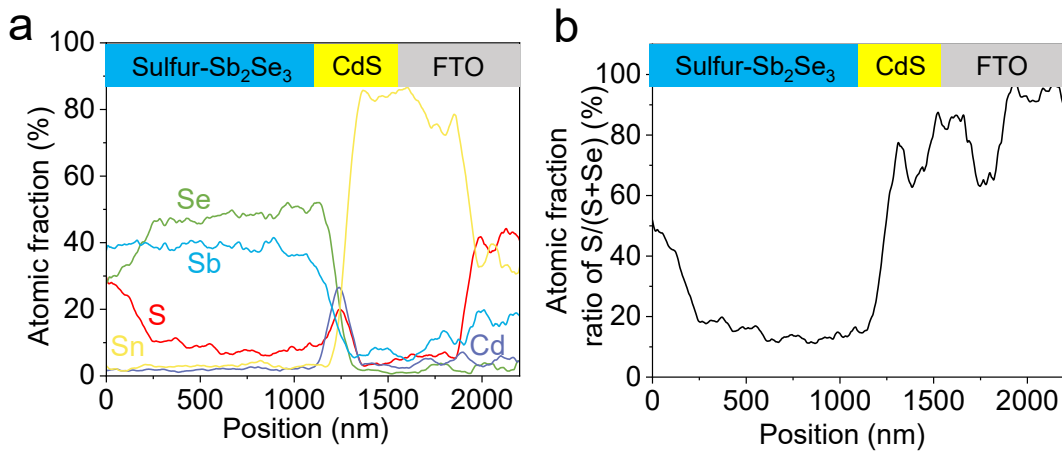


Fig. S7. Elementary composition of the films. a) EDX line scan of Sulfur-Sb₂Se₃; b) Atomic fraction ratio of S/(S+Se) in Sb₂Se₃ films.

Table S1 Effect of annealing temperature on device performance

Temperature/ °C	V _{OC} /V	J _{SC} /mA cm ⁻²	FF/%	PCE/%
370	0.43	28.21	52.75	6.45
360	0.43	27.56	53.81	6.43
350	0.43	27.21	55.36	6.50

Table S2 Effect of annealing time on device performance

Time/min	V _{OC} /V	J _{SC} /mA cm ⁻²	FF/%	PCE/%

10	0.43	27.12	55.36	6.50
20	0.46	29.70	48.98	6.66
30	0.41	29.57	38.05	4.60

Table S3 Effect of the amount of sulfur on device performance

Amount/g	V_{OC}/V	$J_{SC}/mA\ cm^{-2}$	FF/%	PCE/%
0.025	0.41	29.95	54.75	6.71
0.05	0.40	31.31	53.16	6.71
0.1	0.45	30.06	56.23	7.63
0.2	0.44	31.15	54.99	7.53
0.3	0.42	31.48	53.68	7.12
0.4	0.40	30.15	53.76	6.43

Table S4 Effect of the thickness on device performance

Thickness/nm	V_{OC}/V	$J_{SC}/mA\ cm^{-2}$	FF/%	PCE/%
400	0.42	28.81	52.55	6.38
1000	0.45	30.06	56.23	7.63
1200	0.40	31.47	56.41	7.05
1500	0.42	29.75	57.63	7.12

Table S5 Effect of the temperature of sulfur on device performance

Temperature/ °C	V_{oc}/V	$J_{sc}/mA\ cm^{-2}$	FF/%	PCE/%
250	0.45	30.06	56.23	7.63
275	0.40	32.19	54.02	6.90
300	0.38	30.60	56.88	6.59

Table S6 The element proportion of Sulfur-Sb₂Se₃ and Control-Sb₂Se₃

Sb ₂ Se ₃ films	Se (at.%)	S (at.%)	Sb (at.%)	(Se+S)/Sb	S/(Se+S)
Sulfur-Sb₂Se₃	33.0	8.6	21.5	1.93	0.21
Control-Sb₂Se₃	47.5	0	26.3	1.81	0

Table S7 Parameters fitted from electrochemical impedance spectra of devices

Sample	$R_s(\Omega)$	$R_{REC}(\Omega)$
Control-Sb₂Se₃	54.2	15411
Sulfur-Sb₂Se₃	77.74	3046

References

- Y. Zhao, S. Wang, C. Li, B. Che, X. Chen, H. Chen, R. Tang, X. Wang, G. Chen, T. Wang, J. Gong, T. Chen, X. Xiao and J. Li, *Energy & Environmental Science*, 2022, **15**, 5118-5128.
- S. Wang, Y. Zhao, B. Che, C. Li, X. Chen, R. Tang, J. Gong, X. Wang, G. Chen, T. Chen,

J. Li and X. Xiao, *Adv Mater*, 2022, **34**, e2206242.